

Supplemental Material for
Constraints on Climate Sensitivity from Space-Based Measurements of Low-Cloud Reflection

Florent Brient

Department of Earth Sciences, ETH Zürich, Zürich, Switzerland

Tapio Schneider

ETH Zürich, Zürich, Switzerland, and California Institute of Technology, Pasadena, California

(Manuscript received 16 December 2015,

in final form 11 May 2016)

LIST OF TABLES

Table S1. Kullback-Leibler divergences Δ_i for each model for $\delta\alpha_c/\delta\langle T \rangle$ in different frequency bands. The Kullback-Leibler divergences Δ_i indicate how far a model simulation of the covariance of TLC reflection with temperature is from observations (values closer to zero mean simulated covariance is closer to that observed). Bold numbers represent the best simulation in each column. The last row gives the average likelihood (mean of $\exp(-\Delta_i)$ in percent) of climate models for each frequency band. This shows, for example, that the models' simulation of seasonal variability on average is poorer than that of interannual variability. 2

	Model acronym	Deseasonalized	Intraannual	Seasonal	Interannual
1	inmcm4	164.29	95.63	∞	2.15
2	GISS-E2-R	∞	149.51	∞	22.23
3	GISS-E2-H	238.28	∞	28.87	82.24
4	GFDL-ESM2G	7.64	1.52	34.74	7.08
5	GFDL-ESM2M	2.35	1.52	47.29	3.51
6	MRI-CGCM3	0.98	4.33	3.25	0.99
7	IPSL-CM5B-LR	0.40	1.20	6.67	0.42
8	MIROC5	6.09	4.37	17.30	1.88
9	NorESM1-M	5.09	6.43	1.71	0.04
10	bcc-csm1-1	14.98	89.00	116.39	1.55
11	bcc-csm1-1-m	1.26	11.43	45.22	0.42
12	CCSM4	6.61	4.20	19.10	1.33
13	CNRM-CM5	96.23	95.26	∞	6.99
14	MPI-ESM-MR	11.59	4.62	75.99	0.53
15	ACCESS1-3	0.17	1.07	366.65	0.46
16	FGOALS-g2	76.65	24.29	∞	1.41
17	MPI-ESM-P	4.15	6.12	4.69	0.07
18	MPI-ESM-LR	3.92	2.17	8.88	0.87
19	CanESM2	1.07	47.80	1.70	0.75
20	ACCESS1-0	1.92	2.84	42.32	1.60
21	GFDL-CM3	0.43	0.98	16.18	0.07
22	CSIRO-Mk3-6-0	0.81	0.86	155.61	0.43
23	CESM1-CAM5	4.17	2.90	1.17	3.03
24	BNU-ESM	0.74	41.36	1.22	0.57
25	IPSL-CM5A-MR	0.66	0.25	1.44	1.09
26	IPSL-CM5A-LR	0.05	0.72	5.10	0.20
27	FGOALS-s2	0.47	1.05	15.15	1.17
28	HadGEM2-ES	6.38	9.57	90.13	2.70
29	MIROC-ESM	0.50	4.63	128.10	1.44
	Average likelihood (%)	24.46	13.06	4.34	37.51

TABLE S1: Kullback-Leibler divergences Δ_i for each model for $\delta\alpha_c/\delta\langle T \rangle$ in different frequency bands. The Kullback-Leibler divergences Δ_i indicate how far a model simulation of the covariance of TLC reflection with temperature is from observations (values closer to zero mean simulated covariance is closer to that observed). Bold numbers represent the best simulation in each column. The last row gives the average likelihood (mean of $\exp(-\Delta_i)$ in percent) of climate models for each frequency band. This shows, for example, that the models' simulation of seasonal variability on average is poorer than that of interannual variability.

LIST OF FIGURES

11	LIST OF FIGURES	
12	Fig. S1. Frequency with which a location in the annual mean lies within the TLC regions, identi-	
13	fied month-by-month from the mid-tropospheric relative humidity distribution over tropical	
14	oceans in historical simulations with the climate models listed in Table 1. The simulated	
15	months from January 1960 through December 2005 are used to generate the frequencies.	4
16	Fig. S2. Continuation of Figure S1.	5
17	Fig. S3. Constraining ECS using the covariance of intrannual TLC reflection with SST. As Fig. 6,	
18	but for intraannual $\delta\alpha_c/\delta\langle T\rangle$. The correlation coefficient between ECS and intrannual	
19	$\delta\alpha_c/\delta\langle T\rangle$ is $r = -0.40$	6
20	Fig. S4. Constraining ECS using the covariance of seasonal TLC reflection with SST. As Fig. 6, but	
21	for seasonal $\delta\alpha_c/\delta\langle T\rangle$. The correlation coefficient between ECS and seasonal $\delta\alpha_c/\delta\langle T\rangle$ is	
22	$r = -0.49$	7
23	Fig. S5. Constraining ECS using the covariance of interannual TLC reflection with SST. As Fig. 6,	
24	but for interannual $\delta\alpha_c/\delta\langle T\rangle$. The correlation coefficient between ECS and interannual	
25	$\delta\alpha_c/\delta\langle T\rangle$ is $r = -0.68$. (If the outlier models 6 and 23 are removed, the correlation coeffi-	
26	cient increases to $r = -0.82$.)	8

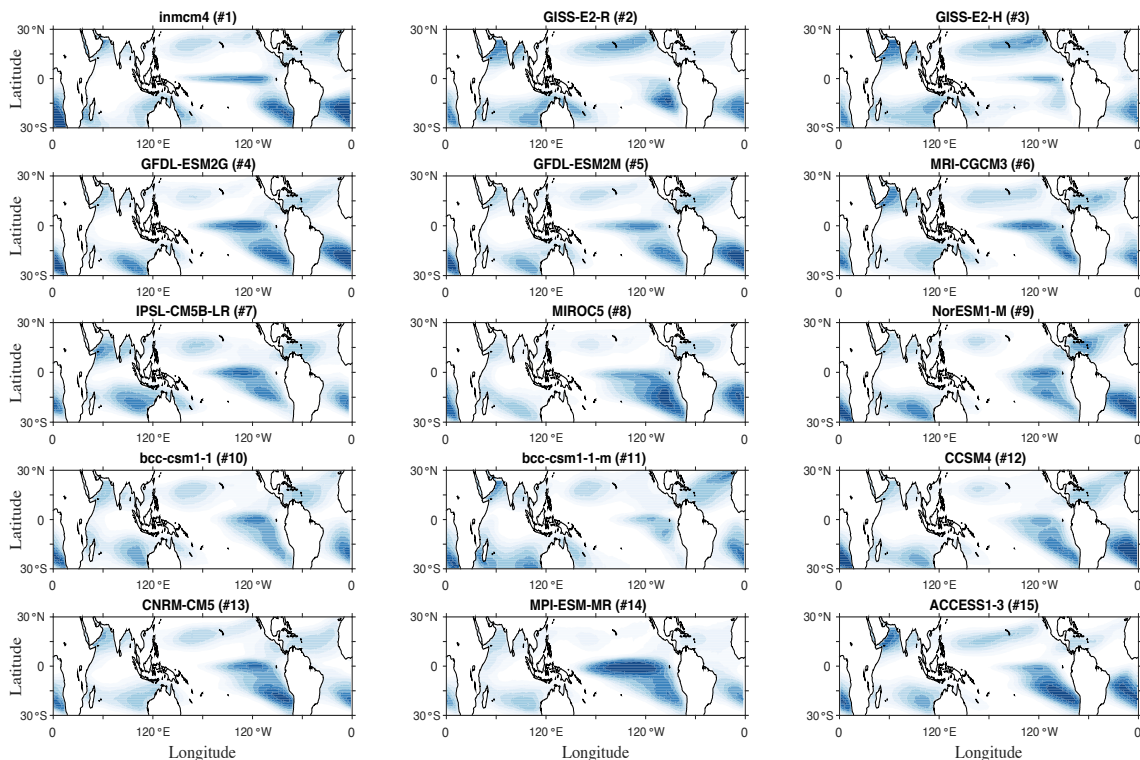


FIG. S1: Frequency with which a location in the annual mean lies within the TLC regions, identified month-by-month from the mid-tropospheric relative humidity distribution over tropical oceans in historical simulations with the climate models listed in Table 1. The simulated months from January 1960 through December 2005 are used to generate the frequencies.

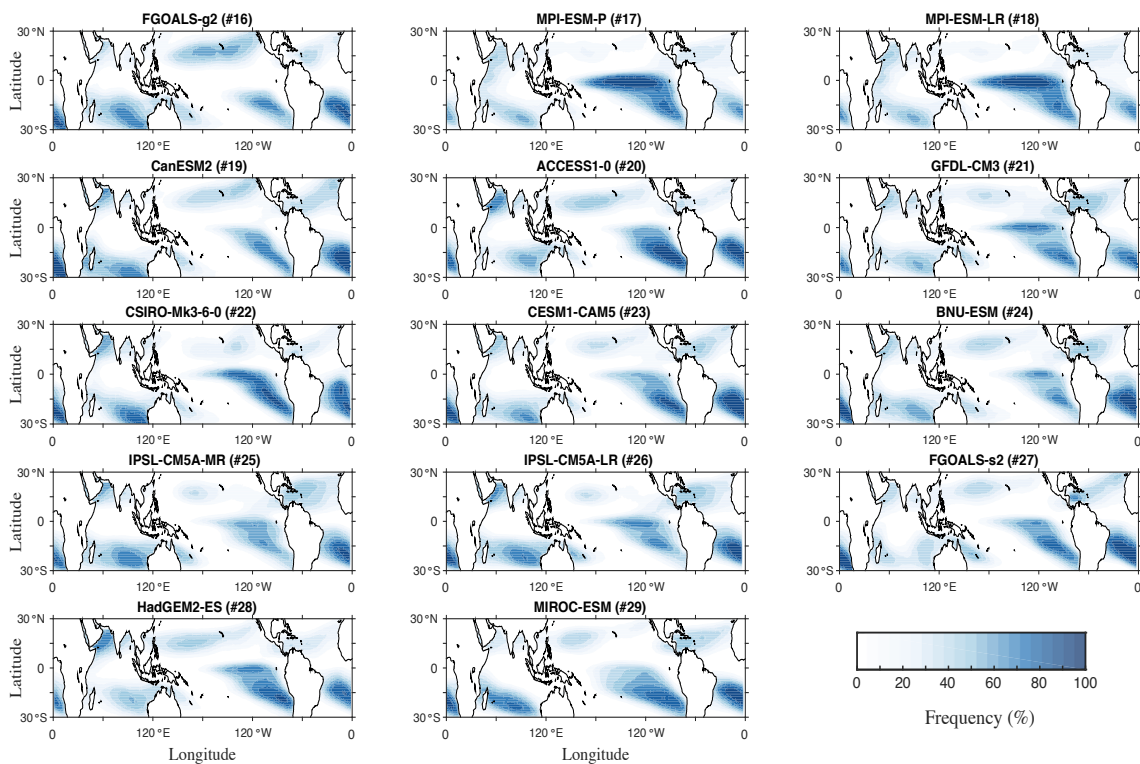


FIG. S2: Continuation of Figure S1.

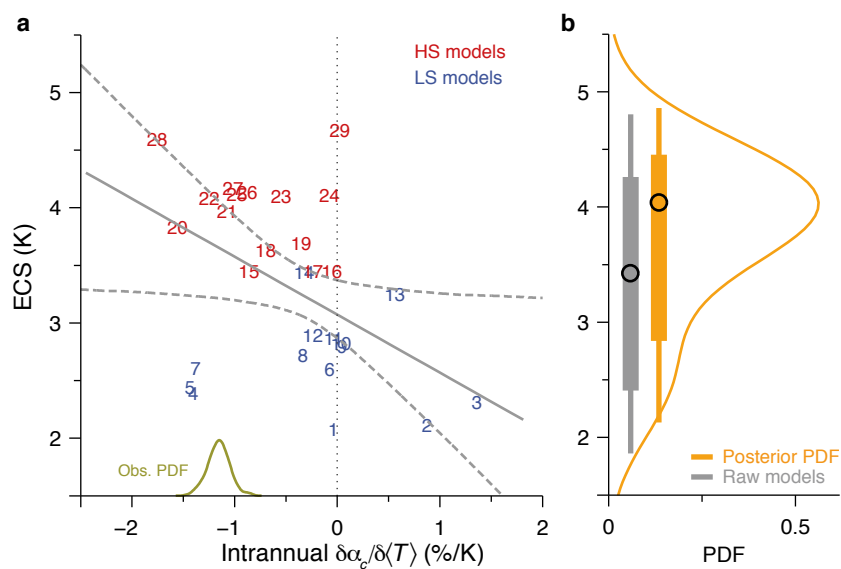


FIG. S3: Constraining ECS using the covariance of intrannual TLC reflection with SST. As Fig. 6, but for intrannual $\delta\alpha_c/\delta\langle T\rangle$. The correlation coefficient between ECS and intrannual $\delta\alpha_c/\delta\langle T\rangle$ is $r = -0.40$.

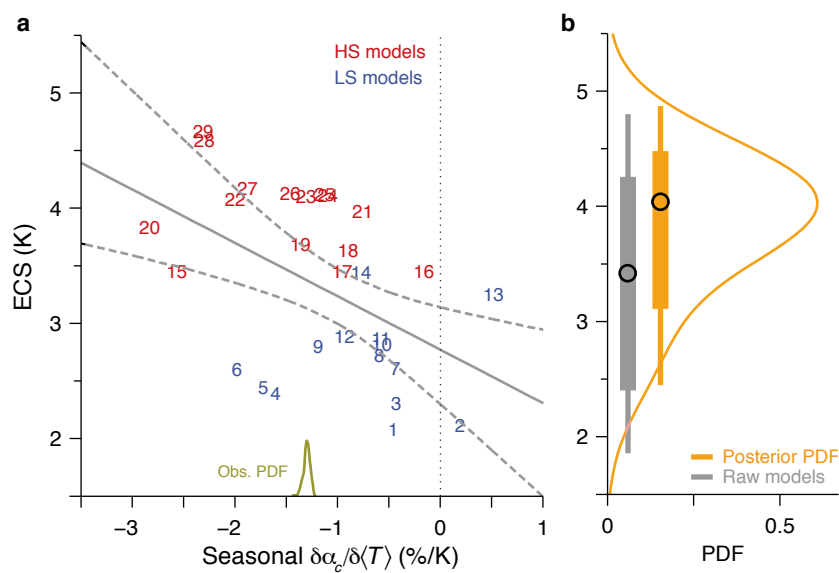


FIG. S4: Constraining ECS using the covariance of seasonal TLC reflection with SST. As Fig. 6, but for seasonal $\delta\alpha_c/\delta\langle T\rangle$. The correlation coefficient between ECS and seasonal $\delta\alpha_c/\delta\langle T\rangle$ is $r = -0.49$.

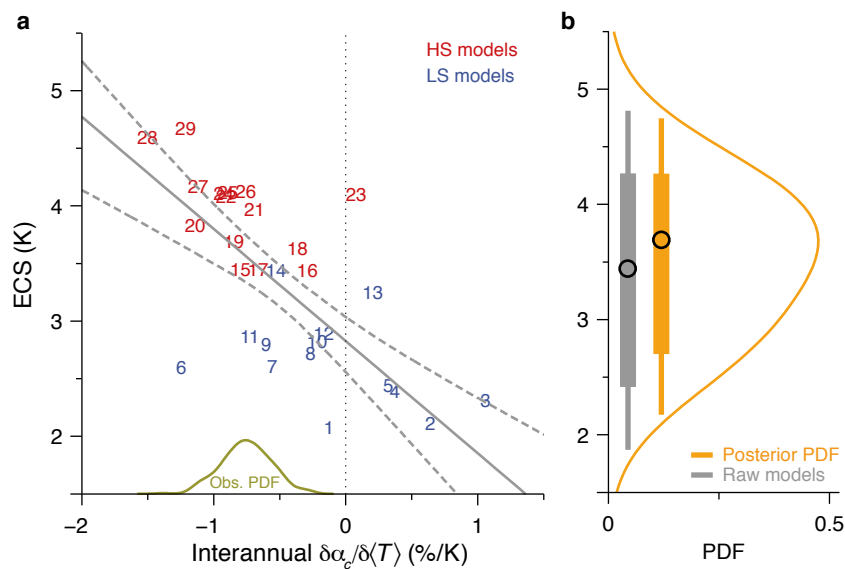


FIG. S5: Constraining ECS using the covariance of interannual TLC reflection with SST. As Fig. 6, but for interannual $\delta\alpha_c/\delta\langle T\rangle$. The correlation coefficient between ECS and interannual $\delta\alpha_c/\delta\langle T\rangle$ is $r = -0.68$. (If the outlier models 6 and 23 are removed, the correlation coefficient increases to $r = -0.82$.)